Supporting Information for:

Heterojunction Constructed From ZIF-8-on-MIL-68(Ga) Precursors for Photocatalytic CO_2 Reduction

Yu Ma[#, a], Qingqing Jiang[#,*, a], Xingyu Li [a], Hao Yu [a], Xiaole Han [a], Yi Liu [a], Qin Li [a], Kangle Lv [a], Juncheng Hu [* a]

[a] School of Chemistry and Materials Science, South-Central Minzu University, Wuhan 430074, China

[#] Yu Ma and Qingqing Jiang contributes equally to this work.

[*] Corresponding author: qqjiang@mail.scuec.edu.cn; jchu@mail.scuec.edu.cn

1. Experimental section

1.1. Materials and reagents

Gallium nitrate hydrate ($Ga(NO_3)_3 \cdot xH_2O$), zinc nitrate hexahydrate ($Zn(NO_3)_2 \cdot 6H_2O$), and 2-methylimidazole were purchased from Aladdin Industrial Corporation. Terephthalic acid (H_2BDC), tetrachloroauric(III) acid tetrahydrate ($HAuCl_4 \cdot 4H_2O$), hexadecyltrimethylammonium bromide (CTAB), N,N-Dimethylformamide (DMF), sodium bicarbonate ($NaHCO_3$), ethanol, and methanol were provided by Sinopharm Chemical Reagent Co., Ltd. All chemicals were of analytical grade and used directly without further purification. Deionized water was used in all experiments.

1.2. Synthesis of MIL-68(Ga)

60 mg of $Ga(NO_3)_3 \cdot xH_2O$ and 60 mg of H_2BDC were dissolved in 30 mL and 10 mL of DMF, which were termed as solution A and solution B respectively. Then solution B was poured into solution A with sonicating for 15 min. Afterward, the mixture was transferred into a 100 mL Teflon-lined stainless autoclave and maintained at a preheated oven at 120 ℃ for 24 h. After cooling down to room temperature, the precipitate was washed with ethanol three times and finally dried at 60 ℃ overnight.

1.3. Synthesis of ZIF-8-on-MIL-68(Ga)

Typically, certain amounts of MIL-68(Ga) (e.g., 50 or 150 mg, respectively) were ultrasonically dispersed in 20 mL of methanol. 5 mg of CTAB and 165 mg of $Zn(NO_3)_2 \cdot 6H_2O$ were added to the above solution and stirred for 1 h. Subsequently, 367.5 mg of 2-methylimidazole was dissolved in 10 mL of methanol and then added into the above mixture and stirred for 10 min. Afterward, the mixture was transferred into a 100 mL Teflon-lined stainless autoclave and kept heating at 90 ℃ for 12 h. After the solvothermal process, the precipitate was washed with ethanol several times and finally dried at 60 ℃ overnight. Products with different amounts of MIL-68 were labeled as ZM-50, and ZM-150. In comparison, pure ZIF-8 was synthesized by the similar method.

1.4. Synthesis of pure ZnO

The pure ZnO were synthesized via calcination of the as-obtained ZIF-8 at 600 ℃ for 4 h with a heating rate of 3 ℃/min.

1.5. Synthesis of pure $ZnGa_2O_4$

The pure $ZnGa_2O_4$ were synthesized via calcination of the as-obtained ZM-150 at 600 ℃ for 4 h with a heating rate of 3 ℃/min.

1.6. Synthesis of ZGO ($ZnGa_2O_4$/ZnO)

The ZGO were synthesized via calcination of the obtained ZM-50 at 600 ℃ for 4 h in air with a heating rate of 3 ℃/min.

1.7. Synthesis of ZGO/Au

50 mg of ZGO-50 (ZGO) was dispersed in 100 mL of H_2O. Then a certain amount of $HAuCl_4$ solution (0.01 g/mL) was added into the above suspension. After stirring for 30 min, 3 mL ice-cooled $NaBH_4$ solution (0.1 M) was rapidly added into the mixture. Then, the mixture was stirred another 30 min. The obtained precipitation was repeatedly washed with deionized water and ethanol and dried at 60 °C overnight in a vacuum, which was denoted as ZGO/Au. A series of ZGO/Au-x samples with different Au loadings were prepared: x = 0.1, 0.25, 0.5, 0.75, and 1 wt. %.

2. Characterizations

Powder X-ray diffraction (XRD) characterizations of the samples were carried out on a Bruker D8 Advance using Cu Kα radiation (λ = 1.5404 Å, Germany). The morphologies of the samples were observed by SU8010 field-emission scanning electron microscope (FESEM, Hitachi, Japan) at a decelerating voltage of 2 kV. The transmission electron microscope (TEM), high-resolution transmission electron microscope (HRTEM), and energy-dispersive X-ray spectroscopy (EDX) were measured on a Thermo Fisher Talos F200X transmission electron microscope operated at 200 kV. Both the X-ray photoelectron spectroscopy (XPS) and valence-band X-ray photoelectron spectroscopy (VB-XPS) were determined by VG Multi lab 2000. The ultraviolet photoelectron spectra (UPS) was performed with the bias of -10 V. The UV-Vis diffused reflectance spectra (DRS) were recorded between 200 and 800 nm on the Cary-5000 spectrophotometer (Agilent) with $BaSO_4$ plate as reference substance. Photoluminescence (PL) measurements were characterized on a Hitachi F-7000 with an excitation wavelength of 255 nm. N_2 adsorption/desorption was measured on an ASAP 2020 PLUS adsorption analyzer (Micromeritics, USA) to obtain the Brunauer-Emmett Teller (BET) surface area and the pore size distribution. $^{13}CO_2$ isotope labeling experiments were conducted under the following conditions: 1.2 g of $NaH^{13}CO_3$, 100 mg catalyst, and 5 mL of H_2SO_4 solution (2M) was injected into the reactor to reacted with $NaH^{13}CO_3$ to produce $^{13}CO_2$ and water vapor in the system. The gas products were quantified by gas chromatography (GC-2014, Shimazu)-mass spectrometry (MS, HPR-20, Hiden Analytic). All the $^{13}CO_2$ was supplied by the $NaH^{13}CO_3$.

3. Photoelectrochemical measurements

All the photoelectrochemical measurements were carried out on a CHI-760E electrochemical workstation (Shenzhen LAMPLIC Science Co. Ltd. China), using a typical three-electrode system, where Pt flake and Ag/AgCl were used as the counter and reference electrode, respectively. The working electrode was prepared as follows: 10 mg of catalyst was dispersed in a mixture containing 970 μL ethanol and 30 μL Nafion. The mixture was uniformly mixed by ultrasonication and then dropped on an ITO glass (1cm × 1 cm). The transient photocurrent was measured using a 3 W LED as the light source ($\lambda \geq 365$ nm) in a 0.5 M Na_2SO_4 aqueous solution as the electrolyte. Electrochemical impedance spectroscopy (EIS) was measure over frequencies ranging from 1 Hz to 10^5 Hz with the initial potential 1.6V.

4. Photocatalytic activity measurements

Photocatalyst activity was tested by photocatalytic CO_2 reduction in porphyry glassware. First, 25 mg of photocatalyst was placed in a Petri dish (Φ = 60 mm). Second, a certain amount of water was added to the Petri dish, and the photocatalyst was dispersed in the water by ultrasonication. It was transferred to a vacuum drying oven and dried overnight to form a uniformly dispersed film and placed in the reactor. Then, 1.2 g of $NaHCO_3$ was added to the glassware. It was sealed and vacuumed (repeated two or three times). Next, 5 ml of H_2SO_4 solution (2M) was injected into the reactor to reacted with $NaHCO_3$ to produce CO_2 and water vapor in the system. A Xe lamp (Perfect-light) was used as simulate sunlight to drive the CO_2 reduction, and after 1 h of irradiation, 1.0 mL of gas was taken and syringed into a gas chromatograph (GC-2014, Shimazu, Osaka, Japan) for product analysis. Circulating water was passed during the photocatalytic process to mitigate the effects of heat from light.

5. Computational details

DFT calculations were conducted through the Vienna ab initio Simulation Package (VASP) with the projector augment wave method[1, 2]. Generalized gradient approximation of the Perdew-Burke-Ernzerhof (PBE) functional was used as the exchange-correlation functional[3]. The Brillouin zone was sampled with 2 × 2 × 1 K points for surface calculation. The cutoff energy was set as 500 eV, and structure relaxation was performed until the convergence criteria of energy and force reached 1×10^{-5} eV and 0.02 eV $Å^{-1}$, respectively. A vacuum layer of 15 Å was constructed to eliminate interactions between periodic structures of surface models. The van der Waals (vdW) interaction

was amended by the zero damping DFT-D3 method of Grimme[4].

The adsorption energy (ΔE_{ads}) of adsorbate adsorption on surface is defined as

$\Delta E_{ads} = E(*adsorbate) - E(*) - E(adsorbate)$

where E(*adsorbate) and E(*) are the total energy of surface systems with and without adsorbate, respectively, E(adsorbate) is the energy of an isolated adsorbate. According to this definition, negative adsorption energy suggests that the adsorption process is exothermic and the adsorption system is thermodynamically stable. Contrarily, a positive value corresponds to an endothermic and unstable adsorption.

The Gibbs free energy was calculated as $\Delta G = \Delta E + \Delta E_{ZPE} - T\Delta S$, where the ΔE, ΔE_{ZPE}, and ΔS are electronic energy, zero-point energy, and entropy difference between products and reactants. The zero-point energies of isolated and absorbed intermediate products were calculated from the frequency analysis[5]. The vibrational frequencies and entropies of molecules in the gas phase were obtained from the National Institute of Standards and Technology (NIST) database[6, 7].

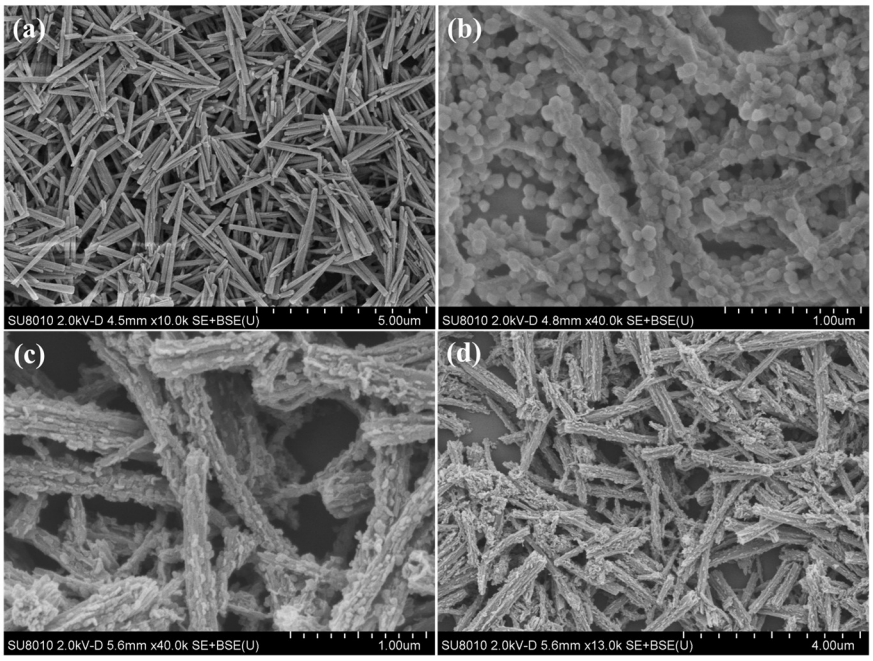

Figure S1. SEM images of (a) MIL-68(Ga), (b) ZIF-8-on-MIL-68(Ga)-50 mg (c) ZIF-8-on-MIL-68(Ga)-100 mg and (d) ZIF-8-on-MIL-68(Ga)-150 mg.

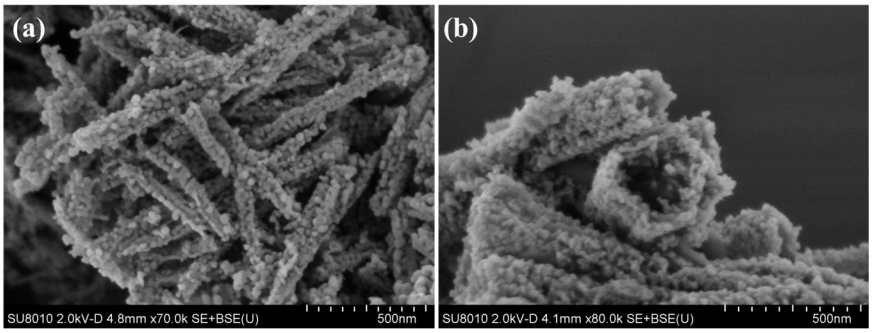

Figure S2. SEM images of ZGO samples.

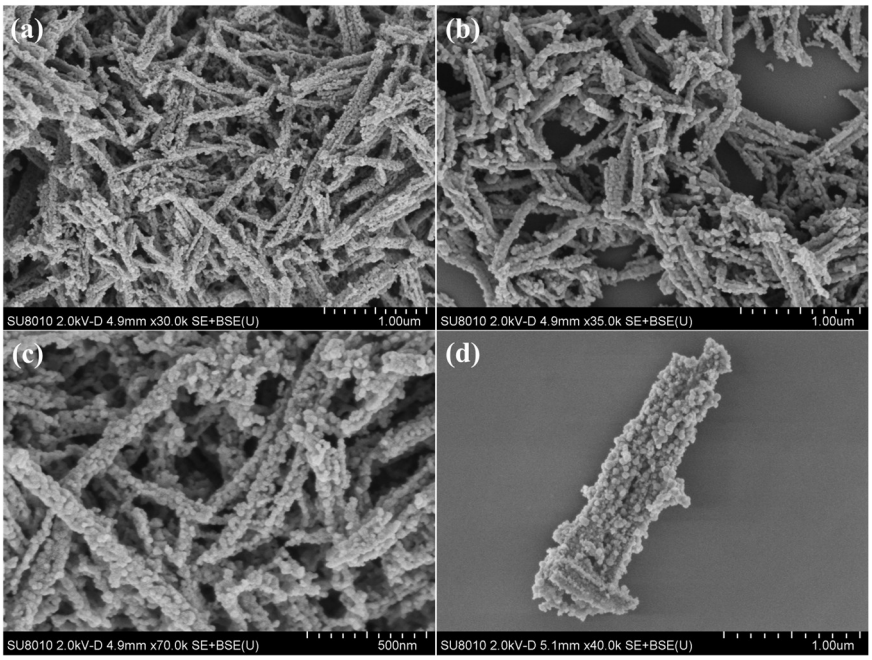

Figure S3. SEM images of ZGO/Au samples.

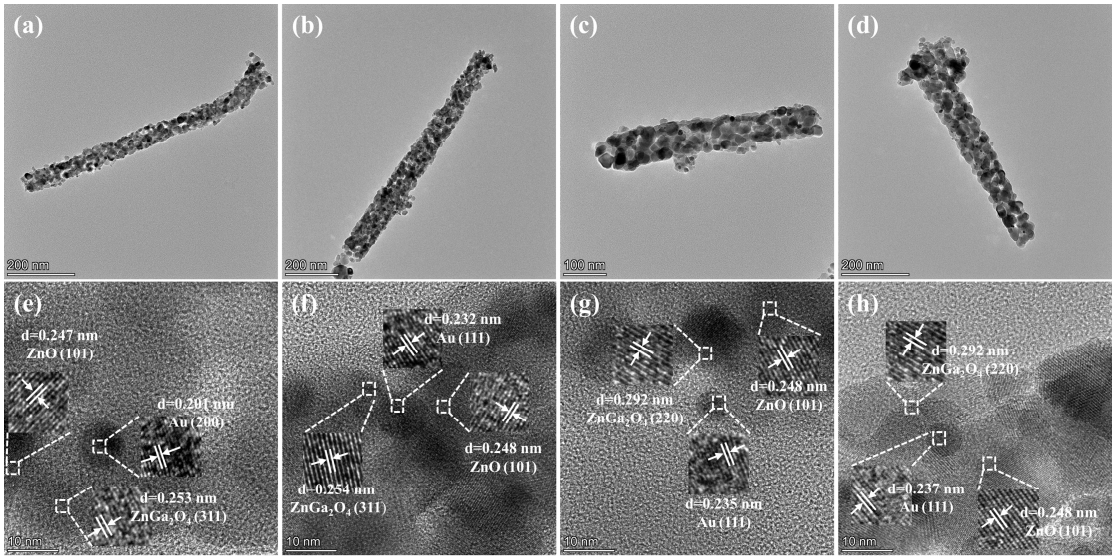

Figure S4. TEM images of (a) ZGO/Au-0.1, (b) ZGO/Au-0.25, (c) ZGO/Au-0.75, and (d) ZGO/Au-1.0. HRTEM images of (e) ZGO/Au-0.1, (f) ZGO/Au-0.25, (g) ZGO/Au-0.75, and (h) ZGO/Au-1.0.

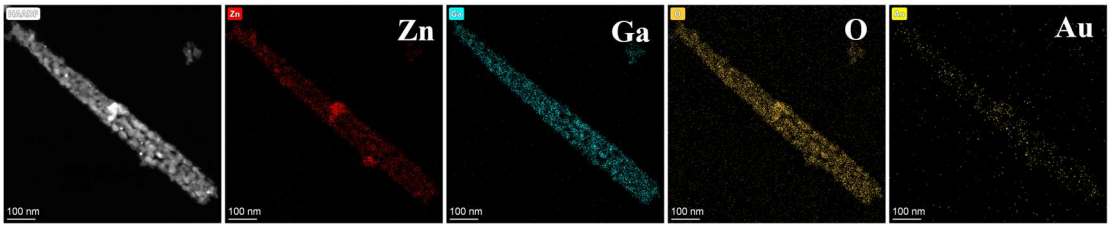

Figure S5. The elemental distribution mapping of ZGO/Au clearly exhibit that the Zn, Ga, O and Au.

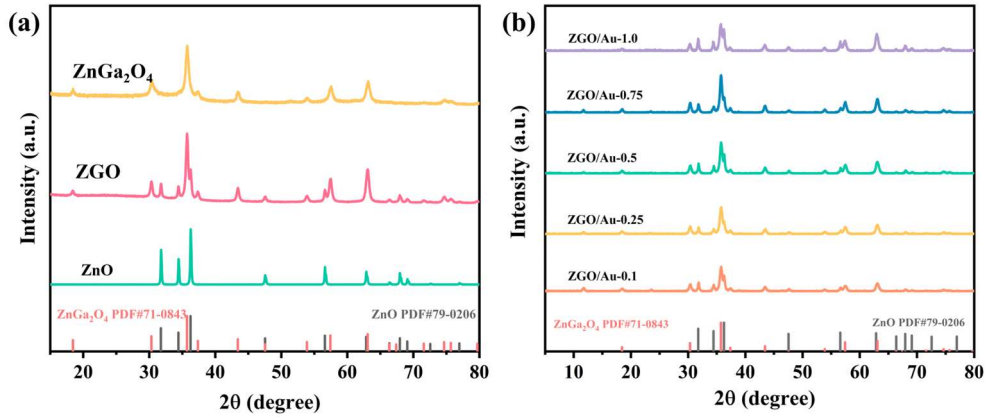

Figure S6. XRD patterns of (a) ZnO, ZGO and $ZnGa_2O_4$, and (b) ZGO/Au.

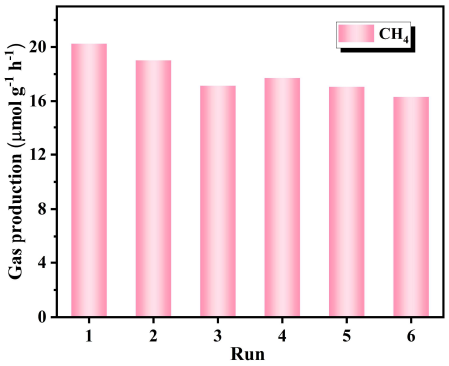

Figure S7. Cycling experiment for photocatalytic CO_2 reduction with ZGO/Au-0.5.

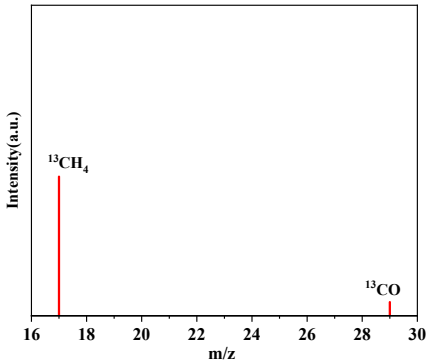

Figure S8. Isotope tracing test of ZGO/Au samples with $NaH^{13}CO_3$.

Table S1. Comparison of photocatalytic CO_2 reduction performance of several similar catalysts that have been reported.

Name	Photocatalysts	CH_4 rate (μmol/g/h)	CO rate (μmol/g/h)	Irradiation condition
1[8]	$ZnGa_2O_4$-10%Ti_3C_2-0.7%Fe	11.81	9.72	500 W Xe lamp (UV light)
2[9]	$Zn_{0.725}Ge_{0.15}Fe_{0.15}Ga_{0.70}O_{2.3}$	/	19.3	300 W Xe lamp (full arc)
3[10]	$ZnGa_2O_4$ nanocube	1.3	/	300 W UV enhanced Xe lamp (200~350 nm)
4[11]	4.5($ZnGa_2O_4$):(Zn_2GeO_4)	5	/	300 W UV enhanced Xe lamp (200~350 nm)
This work	ZGO/Au-0.5	21.1	1.4	300 W Xe lamp (full spectrum)

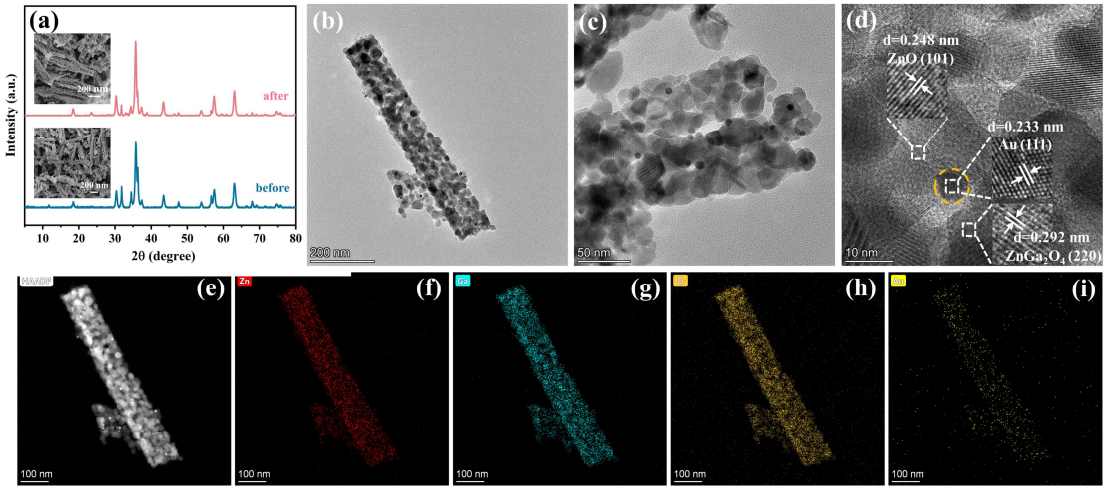

Figure S9. (a) XRD patterns and SEM images of ZGO/Au-0.5 before and after cycling test. (b-c) TEM, (d) HRTEM, and (e-i) EDS images of ZGO/Au-0.5 after cycling test.

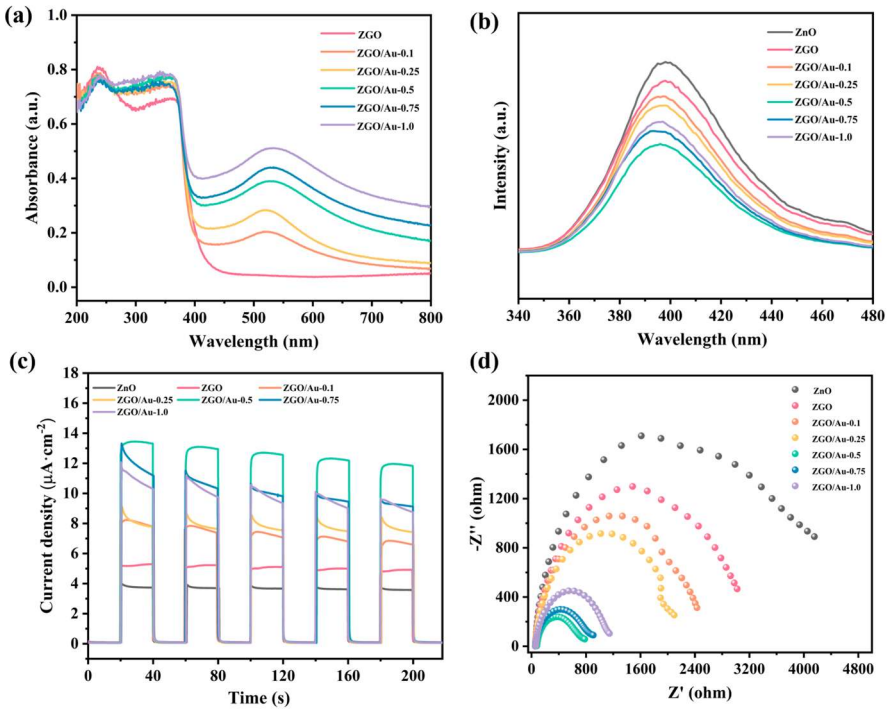

Figure S10. (a) UV-vis DRS spectra, (b) photoluminescence spectra, (c) transient photocurrent response, and (d) EIS of the ZGO/Au-0.5.

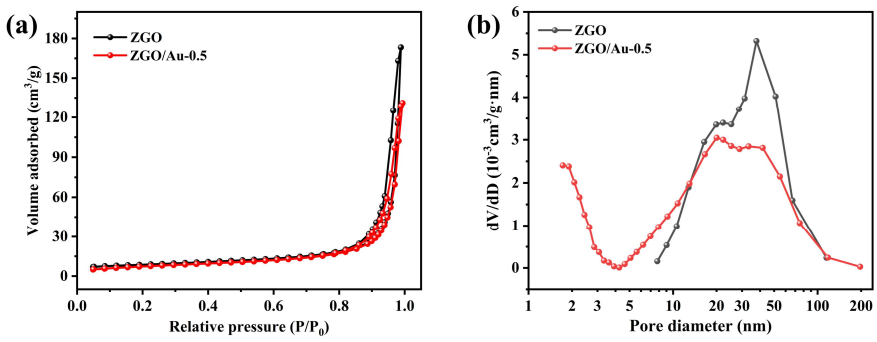

Figure S11. (a) N_2 adsorption-desorption isotherm curves, and (b) pore diameter distribution curves of ZGO and ZGO/Au-0.5.

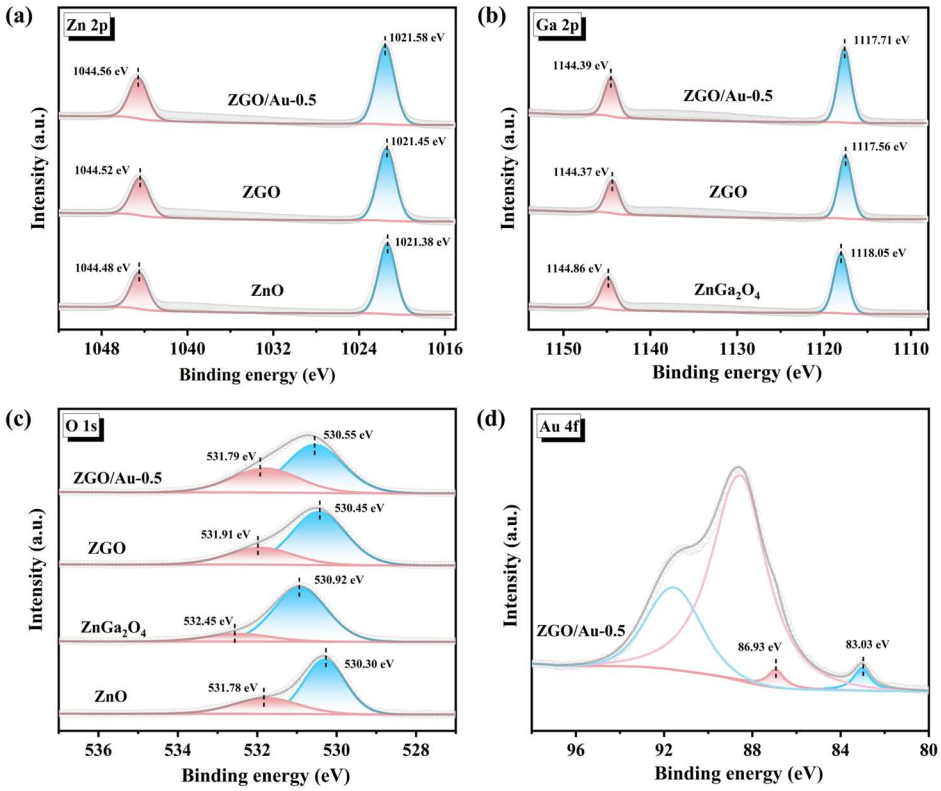

Figure S12. XPS survey spectra of ZnO, $ZnGa_2O_4$, ZGO, and ZGO/Au-0.5.

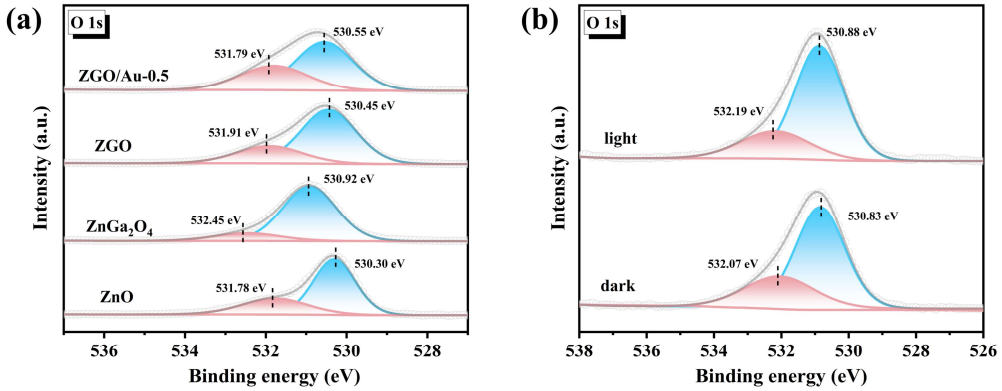

Figure S13. XPS survey spectra for O 1s of (a) ZnO, $ZnGa_2O_4$, ZGO, and ZGO/Au-0.5 and (b) for ZGO/Au-0.5 under light irradiation.

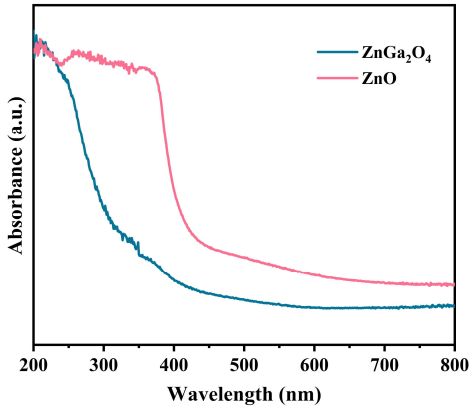

Figure S14. The absorption band edge of $ZnGa_2O_4$ and ZnO.

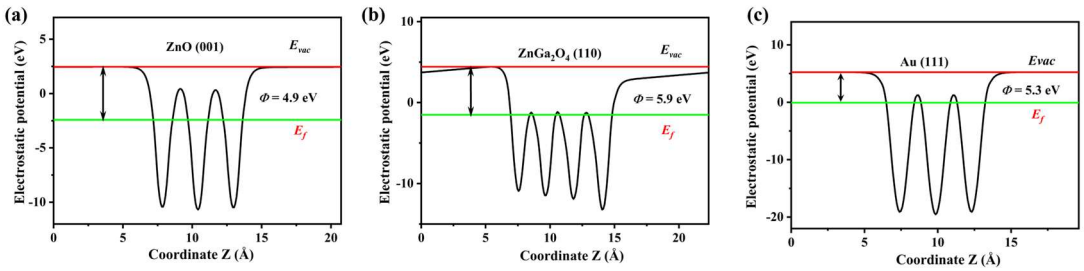

Figure S15. The calculated work functions of ZnO (001), Au (111) and $ZnGa_2O_4$ (110).

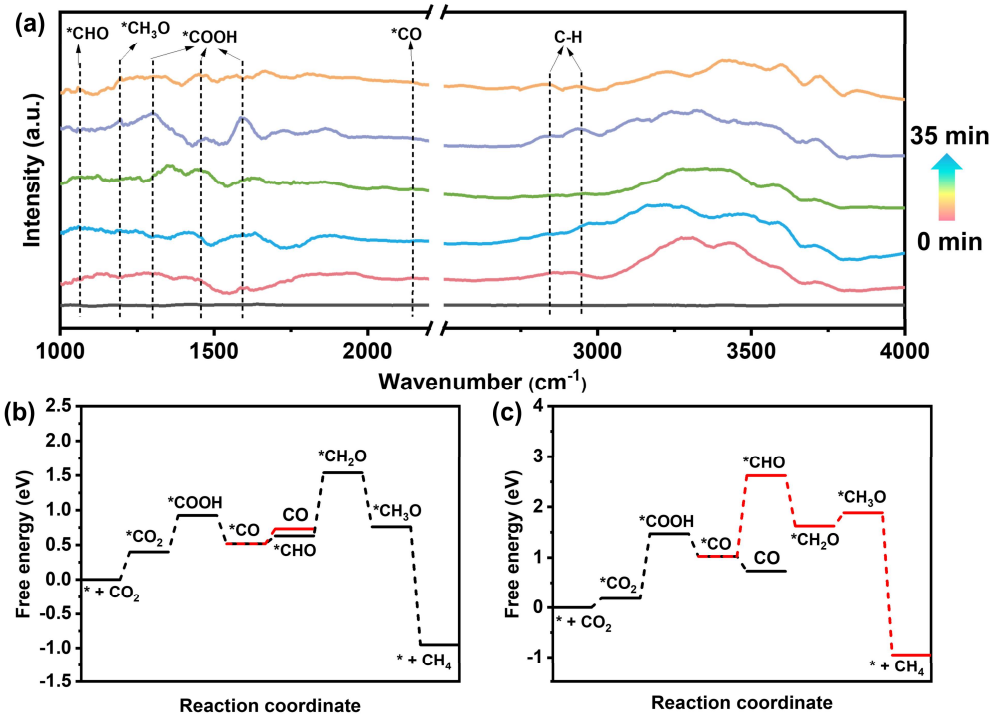

Figure S16. (a) In situ DRIFTS spectrum in photocatalytic CO_2 reduction with ZGO/Au-0.5. Gibbs free energy pathway over (b) ZGO/Au-0.5 and (c) ZGO.

Table S2. BET surface area, pore volume, and average pore diameter of ZGO and ZGO/Au-0.5.

Sample	Surface area [a] (m^2/g)	Pore volume [b] (cm^3/g)	Average pore size [c] (nm)
ZGO	29.25	0.269	44.43
ZGO/Au-0.5	26.69	0.201	29.74

[a.] The surface area is measured with the Brunauer–Emmett–Teller (BET) method. [b.] The pore volume is the single-point total pore volume at $P/P_0 = 0.99$. [c.] The average pore size is calculated using the adsorption branch by Barrett–Joyner–Halenda (BJH) method.

References

(1) Blöchl, P. E. Projector augmented-wave method. *Phys. Rev. B* **1994**, *50* (24), 17953-17979.

(2) Kresse, G.; Joubert, D. From ultrasoft pseudopotentials to the projector augmented-wave method. *Phys. Rev. B* **1999**, *59* (3), 1758-1775.

(3) Perdew, J. P.; Burke, K.; Ernzerhof, M. Generalized Gradient Approximation Made Simple. *Phys. Rev. Lett.* **1996**, *77* (18), 3865-3868.

(4) Grimme, S.; Ehrlich, S.; Goerigk, L. Effect of the damping function in dispersion corrected density functional theory. *J. Comput. Chem.* **2011**, *32* (7), 1456-1465.

(5) Wang, V.; Xu, N.; Liu, J. C.; Tang, G.; Geng, W. T. VASPKIT: A user-friendly interface facilitating high-throughput computing and analysis using VASP code. *Comput. Phys. Commun.* **2021**, *267*.

(6) Noerskov, J. K.; Bligaard, T.; Logadottir, A.; Kitchin, J. R.; Chen, J. G.; Pandelov, S.; Stimming, U. Trends in the Exchange Current for Hydrogen Evolution. *ChemInform* **2005**, *36* (24).

(7) Nørskov, J. K.; Rossmeisl, J.; Logadottir, A.; Lindqvist, L.; Kitchin, J. R.; Bligaard, T.; Jónsson, H. Origin of the Overpotential for Oxygen Reduction at a Fuel-Cell Cathode. *J. Phys. Chem. B* **2004**, *108* (46), 17886-17892.

(8) Shi, Z.; Shi, D.; Zhang, L.; Cao, Y. Regulating the band structure by modifying Ti_3C_2 and doping Fe ions improved photocatalytic activity and selectivity of $ZnGa_2O_4$–Ti_3C_2–Fe for photoreducted CO_2 into CH4. *Journal of Power Sources* **2022**, *535*.

(9) Liang, J.; Chai, Y.; Li, L.; Li, D.; Shen, J.; Zhang, Y.; Wang, X. Germanium and iron double-substituted $ZnGa_2O_4$ solid-solution photocatalysts with modulated band structure for boosting photocatalytic CO_2 reduction with H_2O. *Appl. Catal. B Environ.* **2020**, *265*.

(10) Yan, S.; Wang, J.; Gao, H.; Wang, N.; Yu, H.; Li, Z.; Zhou, Y.; Zou, Z. An Ion-Exchange Phase Transformation to $ZnGa_2O_4$ Nanocube Towards Efficient Solar Fuel Synthesis. *Adv. Funct. Mater.* **2012**, *23* (6), 758-763.

(11) Yan, S.; Wang, J.; Gao, H.; Wang, N.; Yu, H.; Li, Z.; Zhou, Y.; Zou, Z. Zinc Gallogermanate Solid Solution: A Novel Photocatalyst for Efficiently Converting CO_2 into Solar Fuels. *Adv. Funct. Mater.* **2012**, *23* (14), 1839-1845.